EXPERIMENT INVESTIGATION OF THREE-DIMENSIONAL ISOLATOR AND EARTHQUAKE RESPONSE OF A NUCLEAR POWER PLANT

H. Xu(1), WF. He(2), SP. Li(3), J. Yang(4)

(1) Lecturer, Shanghai University, xuhaoxy08@shu.edu.cn
(2) Associate professor, Shanghai University, howunfu@shu.edu.cn
(3) Professor, Shanghai Nuclear Engineering Research & Design Institute, lisp@snerdi.com.cn
(4) Senior engineer, Shanghai Nuclear Engineering Research & Design Institute, yangjie@snerdi.com.cn

Abstract

Nuclear energy is an important energy source for human and the safety of nuclear power plant is the precondition of the entire nuclear system. Seismic isolation is an efficient method to protect structure from strong earthquakes. Strong vertical ground motions and structural damage have been observed in epicenter regions and near-fault areas. While conventional seismic isolation systems are not designed to reduce the structural responses in the vertical direction. It is very necessary to control the vertical response of nuclear power plant. A novel three-dimensional isolator was proposed in which the lead rubber bearings were installed with inclination. And the asymmetric hysteretic model was illustrated. The stiffness in loading process and unloading process are different and the hysteretic curve has a shape of asymmetric quadrangle. A static test of the model device consists of three LRB300 was conducted including compression, shear, and bi-directional loading test. The test results and theory values are close. The three-dimensional isolator has similar horizontal behavior with conventional LRB. The vertical hysteretic curves are asymmetric and have the shape of spindle. With different horizontal deformation the test curves are similar, showing that the horizontal deformation has little influence on the vertical behavior. The hysteretic curves in bi-directional cases are close with the corresponding compression and shear cases, which indicates that the vertical behavior is decoupled with the horizontal behavior. A numerical model of an AP1000 nuclear power plant including containment and internal equipment was established. The three-dimensional isolation design and the earthquake analysis were accomplished. Four artificial ground motions were generated according to the RG1.60 response spectrum. The horizontal responses of the three-dimensional isolated structure and the horizontal isolated structure are close. In vertical direction, the three-dimensional isolated structure reduced acceleration responses while the horizontal isolated structure and the fixed structure amplified vertical accelerations. The pressure of the three-dimensional isolator was obviously reduced. The pressure of horizontal isolators were larger than 1 MPa while the three-dimensional isolators remained compressed under 0.9 g input. The proposed three-dimensional isolator can significantly improve the seismic safety of nuclear power plant.

Keywords: three-dimensional isolation, nuclear power plant, static test, earthquake response

1. Introduction

Nuclear energy is an important energy source for human and the safety of nuclear structure is the precondition of entire nuclear system. Seismic isolation is an efficient method to protect structure from strong earthquake while conventional seismic isolation systems are not designed to reduce the structural responses in the vertical direction (Architectural Society of Japan, 2006). However, strong vertical ground motions and structural damage have been observed in epicentral regions and near-fault areas (Papazoglou, and Elnashai, 1996). It is very necessary to control vertical response of nuclear structure.

Fujita (1996) proposed a new device using disc springs as vertical isolator and rubber bearing as horizontal isolator. The first application of 3D isolation is the retrofitting of Pestalozzi School using thick rubber bearing (Garevski M, 2000). A kind of hydraulic cylinder bearing and isolation system with rocking suppression device was introduced by Kato, A (2002). A new device using metal bellows and rubber bearing was put forward by Seitaro O (2003). Meng QL. (2007) proposed a semi-active control system using disc spring and hydraulic cylinder. Device using rubber bearing with SMA wire and disc spring was introduced by Liu HQ. (2008). A kind of rocking-suppression bearing using thick rubber bearing combined with cable wire was proposed by Zhang YS. (2009). A three-dimensional isolated RC apartment were built in Tokyo (Tomizawa T, 2012). The isolation device includes rubber bearing and air spring, and the vertical isolation period is one second. A new device consisting of disc spring, metal damper and rubber bearing was proposed and applied in bridges by Jia JF. (2012). Wei LS. (2014) conducted a shaking table test on a separate type three-dimensional isolation system.

2. Mechanical Behavior of the 3D Isolator

2.1 Components and Mechanical Model

A new three-dimensional isolator including lead rubber bearings, friction sliding plates, and restrainers was proposed (Liu WG., 2018). As shown in Figure 1, in the device rubber bearings are installed with inclination. Under vertical load, the vertical deformation would transform to oblique sliding and shear deformation of the inclined bearing. Under horizontal load, the restrainers transmit shear force and make the inclined bearings not overburden, while horizontal bearing performs as conventional seismic isolators.

The load condition of the incline rubber bearing is displayed in Figure 2(a). The vertical load decomposed into friction force, shear force and axial force of the inclined bearings. In the loading and unloading process, the direction of the friction force is different.

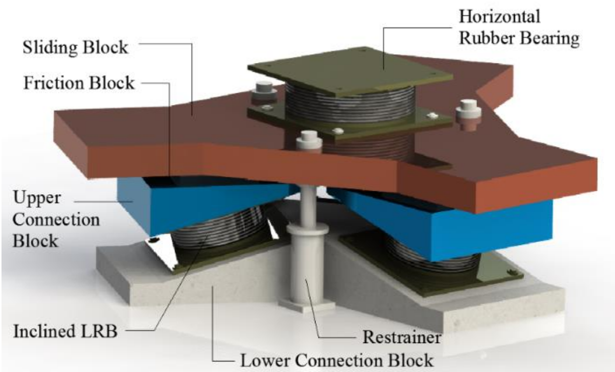

Fig. 1 - Sketch and Deformation of 3D Seismic Isolator

The vertical stiffness and yielding load of the proposed isolator can be obtained from Equation 1 to Equation 3. The hysteretic model is presented in Figure 2(b). The stiffness in loading process is larger than the stiffness in unloading process due to the reverse of friction force. The hysteretic loop has a shape of asymmetric quadrangle.

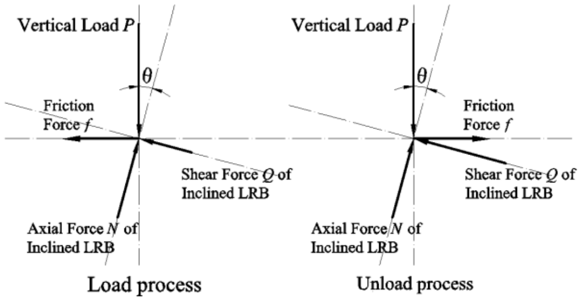

(a) load condition

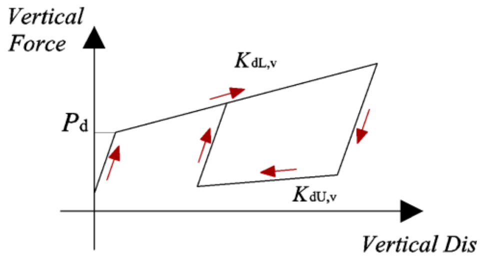

(b) mechanical model

Fig. 2 - Load condition and mechanical model of proposed isolator

The vertical post-yield loading stiffness is:

$$K_{\mathrm{dL,V}} = \frac{n \cdot \mathrm{d}P}{\mathrm{d}\Delta_{\mathrm{v}}} = \frac{n \cdot K_{\mathrm{d}} \cdot K_{\mathrm{v}}}{K_{\mathrm{v}} \cdot (\sin^2\theta - \mu \cdot \sin\theta \cdot \cos\theta) + K_{\mathrm{d}} \cdot (\cos^2\theta + \mu \cdot \sin\theta \cdot \cos\theta)} \tag{1}$$

The yielding load is

$$P_{\mathrm{d}} = \frac{n \cdot Q_{\mathrm{d}}}{\sin\theta - \mu \cdot \cos\theta} \tag{2}$$

The vertical post-yield unloading stiffness of the 3D OSFSI can be obtained with the same method and is

$$K_{\mathrm{dU,V}} = \frac{n \cdot \mathrm{d}P}{\mathrm{d}\Delta_{\mathrm{v}}} = \frac{n \cdot K_{\mathrm{d}} \cdot K_{\mathrm{v}}}{K_{\mathrm{v}} \cdot (\sin^2\theta + \mu \cdot \sin\theta \cdot \cos\theta) + K_{\mathrm{d}} \cdot (\cos^2\theta - \mu \cdot \sin\theta \cdot \cos\theta)} \tag{3}$$

2.2 Static Test

A static test of model device was conducted to investigate the mechanical behavior of the three-dimensional isolator. The test model consists of three inclined lead rubber bearings with diameter 300 mm and one lead rubber bearing with diameter 400 mm. The inclination angle is 10 degrees. The friction materials of the sliding surfaces are PTFE and steel. Three restrainers are established to make the inclined bearings move up and down. The contact surface of restrainers and sliding block is also PTFE and steel. So the impact of vertical friction force can be ignored.

Bidirectional compression-shear test was performed using an electro-hydraulic servo loading system, as shown in Figure 3(a). The test device is displayed in Figure 3(b).

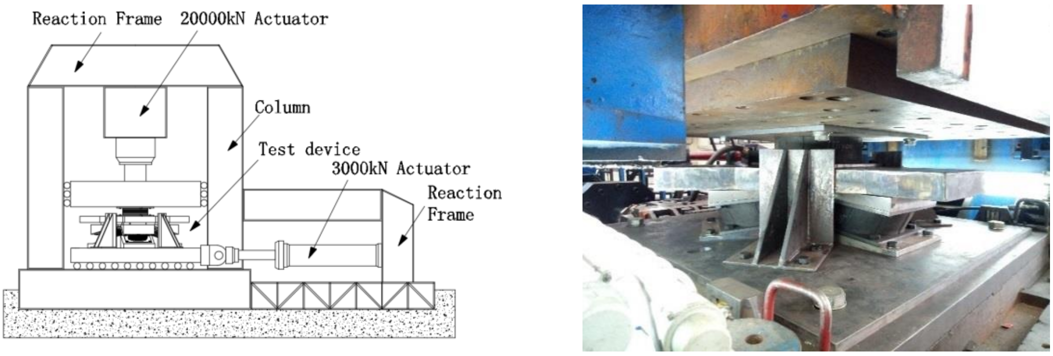

(a) Electro-hydraulic servo loading system (b) Test device

Fig. 3 - Static test system of three-dimensional isolator

Table 1 – Load cases

Cases	Horizontal deformation (mm)	Vertical deformation (mm)	Test type
1	±50	3.5	Shear test
2	±100		
3	0	5.3±3.5	Compression test
4	25	5.3±3.5	
5	50	5.3±3.5	
6	75	5.3±3.5	
7	±50	5.3±3.5	Bidirectional test
8	0	0~24	Ultimate compression test

The detail load cases are presented in Table 1. In both vertical and horizontal directions deformation control was used. The target deformation is determined by shear strain of the horizontal and inclined bearings. Case 1 and Case 2 are shear test cases. Unlike conventional compression-shear test of rubber bearing, the vertical load is designed by deformation here. Case 3 to Case 6 are compression test cases. In each case the horizontal bearing was performed a shear deformation before vertical loading. Case 7 is a bidirectional test. The vertical and horizontal loading were conducted simultaneously. Case 8 is an ultimate compression test. The shear strain of the inclined bearings is larger than 350%.

The horizontal test results of Case 1 and Case 2 are shown in Figure 4(a) and (b). The hysteretic curves present as a fusiform shape, which is similar with the shear loop of traditional lead rubber bearing. The sliding block and the inclined bearings are not fixed. So the sliding block would have a micro rocking deformation under horizontal load. This leads to a stiffness change under large shear deformation. In Case 1, when the shear strain ranges from 50% to 100%, the stiffness got a little larger. In Case 2, the shear strain is 200%, and the curve is larger in the two ends while smaller in the middle.

The vertical curves of Case 3 to Case 6 are shown in Figure 4(c) to Figure 4(f), respectively. The target of vertical deformation ranges from 1.8 mm to 8.8 mm. The corresponding shear strain of the inclined bearing range from 30% to 130%. The horizontal deformation is 0, 25 mm, 50 mm, and 75 mm, respectively. Due to the assembly tolerance of the test device and the control error of the test machine, the actual deformation in each case has some difference. The hysteretic loops are asymmetric and have a shape of ellipse. The loading stiffness are significantly larger than the unloading stiffness. The curves in each case are similar, which indicates that the horizontal deformation has little influence on vertical behavior.

Figure 4(g) and Figure 4(h) presented a comparison of the results of bidirectional test and the corresponding unidirectional test. When the target deformation is same, both the horizontal and vertical hysteretic curves are close. The horizontal and vertical behavior can be considered independent and decoupled.

The hysteretic curve of ultimate compression test is displayed in Figure 4(i). The maximum vertical deformation is 24 mm. And the corresponding shear strain of the inclined bearing is 350%. The three-dimensional isolator remained stable and the hysteretic loop was smooth during the load. When the vertical deformation is larger than 13 mm (corresponding shear strain 200%), the stiffness got bigger due to the hardening effect of rubber.

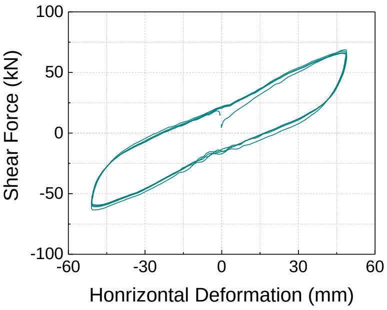

(a) Case 1

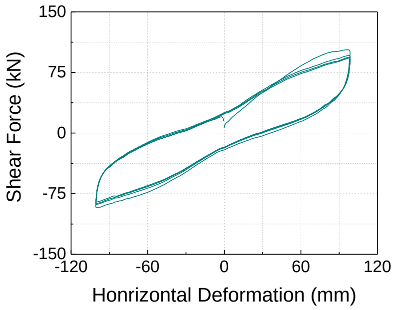

(b) Case 2

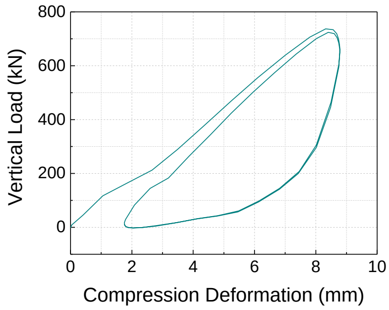

(c) Case 3

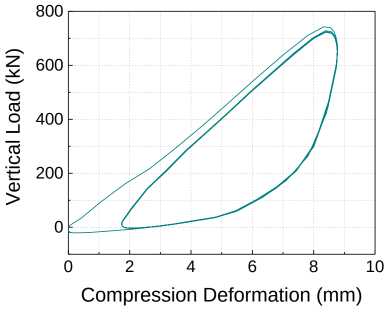

(d) Case 4

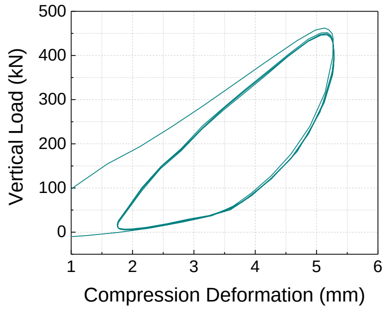

(e) Case 5

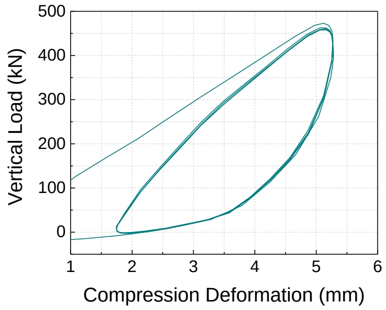

(f) Case 6

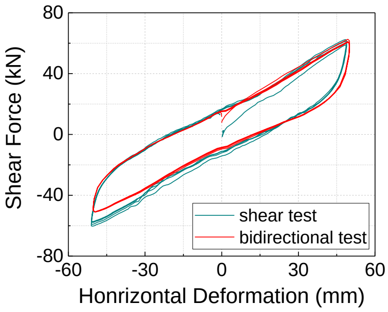

(g) Case 7

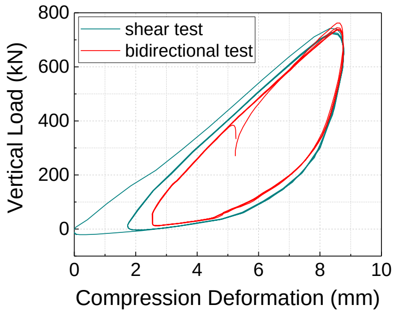

(h) Case 8

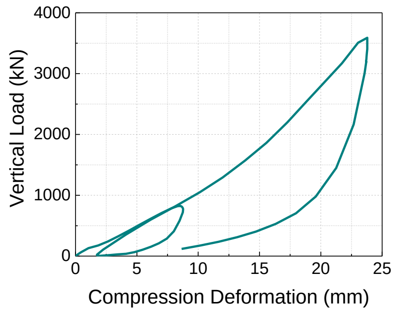

(i) Case 9

Fig. 4 - Test results

3. Seismic Analyses of 3D Isolated Nuclear Power Plant

3.1 Seismic Isolation Design

A particle system model of a nuclear power plant was established. The calculation model includes the containment structure and the internal equipment (Li ZX., 2005). A coupling relationship was assigned to the mass points to simulate the structural-equipment interaction. The detail structure of the nuclear plant and the numerical model are shown in Figure 5.

In the isolation layer 131 three-dimensional isolators and rocking suppression system were installed. In each isolator the diameter of the horizontal bearing is 1200 mm and the diameter of the three inclined bearing are 800 mm. The inclination angle is 20 degrees, and the friction coefficient is 0.05. The detail parameters of the three-dimensional isolator were listed in Table 2. An equivalence principle was used when calculating the vertical post yield stiffness. The stiffness is considered as the average value of loading and unloading stiffness.

Four ground motions were selected in this study. The motions were generated artificially and were consistent with the RG1.60 response spectrum (NRC, 2014). The input peak ground accelerations (PGAs) are 0.3 g, 0.6 g and 0.9 g. The response spectra of the selected waves are displayed in Figure 6.

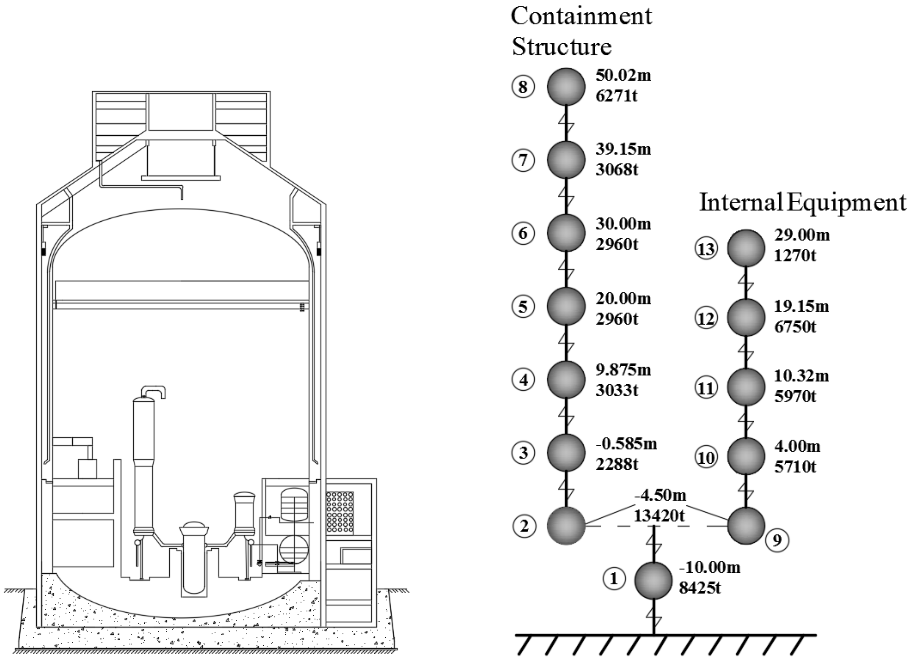

Fig. 5 - Numerical model of nuclear power plant structure

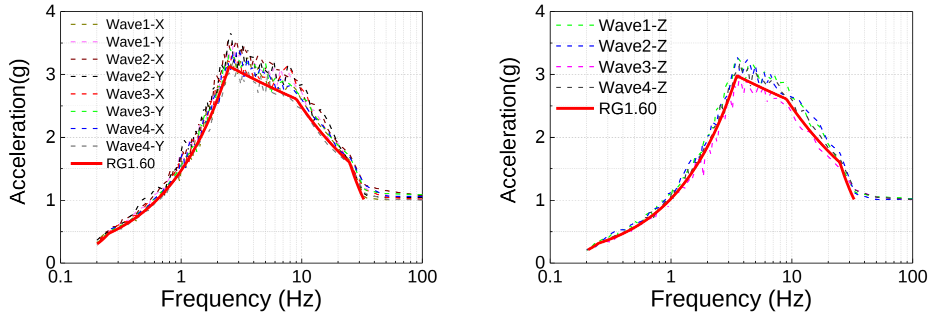

Fig. 6 - Comparison of RG1.60 spectra and response spectra of generated waves

Table 2 – Details and mechanical properties of isolation devices

Device	Parameters	Value
Inclined LRB	Compression stiffness (kN/mm)	6787
	Lateral post yield stiffness (kN/mm)	2.374
	Lateral yielding strength (kN)	362
Three-dimensional isolator	Horizontal stiffness (kN/mm)	1377
	Horizontal post yield stiffness (kN/mm)	0.691
	Horizontal yielding strength (kN)	68.7
	Vertical post yield stiffness (kN/mm)	18.0
	Vertical yielding strength (kN)	698.6
	Rotational stiffness (kN/mm)	1.62×10^{11}

3.2 Earthquake Responses

The peak accelerations of four mass points were displayed to evaluate the earthquake response of three-dimensional isolated nuclear plant. The responses of three-dimensional isolated building, horizontal isolated building, and fixed base building were compared in Table 3. Node 1 is on the isolation layer. Node 8 is on the top of containment. Node 13 and Node 10 are on the top and bottom of the steam generator, respectively.

In horizontal directions, the accelerations of the three-dimensional isolated structure and the horizontal isolated structure are close, and are much smaller compared with the acceleration of the fixed base structure. In some cases, the accelerations of the three-dimensional isolated structure are larger than that of the horizontal isolated structure. This is supposed to be the result of rocking effect. In vertical directions, the horizontal isolated structure amplified acceleration response while the three-dimensional isolated structure can significantly reduce acceleration response. With larger input PGA, more significant damping effect can be observed. The responses of Node 8 for the three-dimensional isolated structure under 0.9 g input are even smaller than that of the fixed base structure under 0.3 g input.

The acceleration spectra of Node 13 under Wave 3 are shown in Figure 7. The horizontal spectra of three-dimensional isolated structure and horizontal isolated structure are close. While the vertical spectra of horizontal isolated structure and fixed base structure are close. The predominant periods of the three-dimensional isolated structure are larger in both horizontal and vertical directions. The vertical spectra of the three-dimensional isolated structure can be enveloped by the spectra of the fixed base structure.

The widely used rubber bearing has larger compression stiffness and low tension stiffness. One of the concerns about seismic isolated building is the rocking deformation and tensile collapse of rubber bearing. For an isolated building with large aspect ratio, the corner bearing is easy to be tensioned under three-dimensional ground motions. The three-dimensional system has a low vertical stiffness, which would lead to a huge rocking deformation. While it would sufficiently reduce vertical response and compression pressure of isolator. In the actual three-dimensional nuclear structure, a series of rocking suppression system were established to provide rotational stiffness. So the three-dimensional isolators would have close responses.

A comparison on the vertical stress of horizontal isolators and three-dimensional isolators was shown in Figure 8 (a) to (c). Isolator A is the centre bearing. Isolator B to Isolator E are the four corner bearings. The designed pressure for each bearing is 5 MPa. For the horizontal isolators, the vertical stress varies with isolator number. The stress of corner isolators has a larger range than the centre isolator. Under 0.3 g PGA input, the isolators remained compressed. Under 0.6 g PGA input, the corner isolators are tensioned. And under 0.9 g PGA input, the stress of corner isolators is beyond tensile stress limitation. For the three-dimensional isolators, the stress of each isolator is close. Under 0.9 g PGA input, all the three-dimensional isolators remain compressed. The vertical hysteretic loops of Isolator A are presented in Figure 8 (d) to (f). The maximum vertical deformations of Isolator A are 19 mm, 57 mm, and 104 mm, respectively under 0.3 g input, 0.6 g input, and 0.9 g input.

Table 3 - Average acceleration of main points

Node No.	Structure	*PGA* 0.3g			*PGA* 0.6g			*PGA* 0.9g		
		X	Y	Z	X	Y	Z	X	Y	Z
Node 1	3Diso	0.18	0.20	0.28	0.33	0.32	0.44	0.72	0.71	0.70
	Hiso	0.16	0.19	0.36	0.33	0.32	0.67	0.67	0.62	1.11
	Fixed	0.30	0.30	0.30	0.60	0.60	0.60	0.90	0.90	0.90
Node 8	3Diso	0.64	0.69	0.64	0.83	0.96	0.87	1.16	1.25	0.98
	Hiso	0.48	0.65	1.71	0.61	0.81	3.06	1.04	1.20	4.64
	Fixed	2.43	2.35	1.46	4.26	4.80	2.74	6.39	7.20	4.11
Node 13	3Diso	0.27	0.38	0.31	0.43	0.53	0.42	0.78	0.83	0.69
	Hiso	0.27	0.30	0.44	0.48	0.77	0.86	0.97	2.20	1.46
	Fixed	1.12	1.24	0.44	1.92	2.43	0.80	2.88	3.64	1.20
Node 10	3Diso	0.38	0.32	0.44	0.48	0.43	0.53	0.84	0.75	0.75
	Hiso	0.31	0.29	0.83	0.56	0.55	1.63	0.90	1.02	2.53
	Fixed	1.99	1.84	0.69	4.10	3.36	1.33	6.15	5.05	1.99

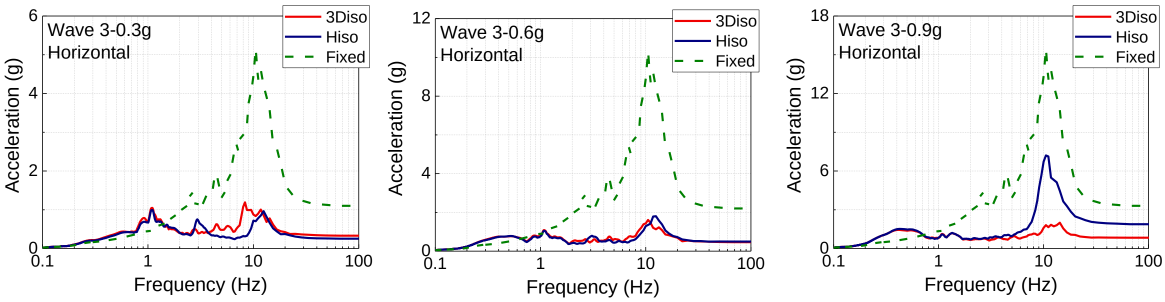

(a) 0.3 g input, horizontal (b) 0.6 g input, horizontal (c) 0.9 g input, horizontal

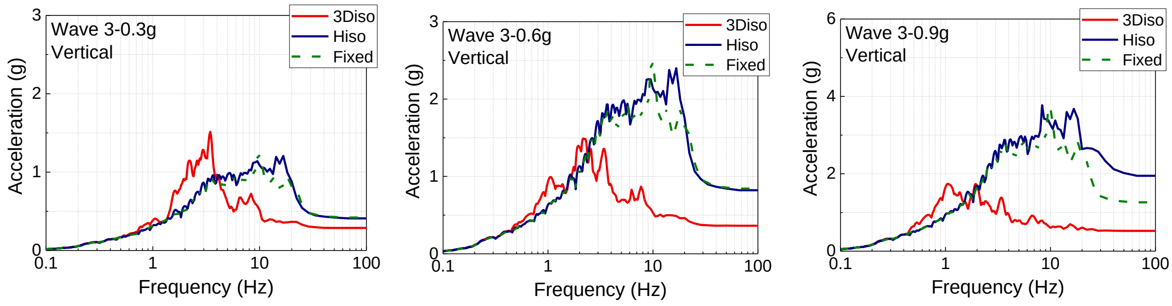

(d) 0.3 g input, vertical (e) 0.6 g input, vertical (f) 0.9 g input, vertical

Fig. 7 - Acceleration response spectra of internal equipment (Node 13)

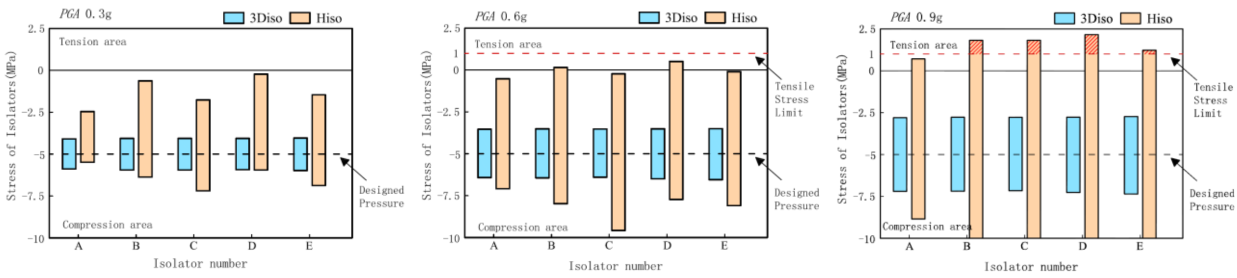

(a) average stress, 0.3 g input (b) average stress, 0.6 g input (c) average stress, 0.9 g input

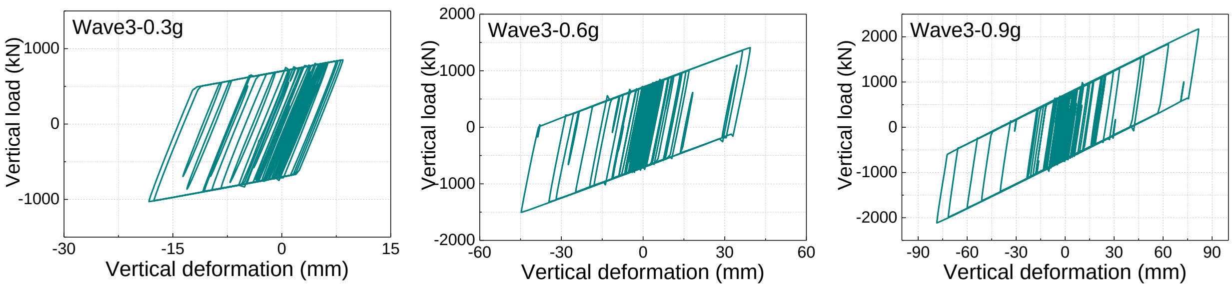

(d) hysteretic loop, 0.3 g input (e) hysteretic loop, 0.6 g input (f) hysteretic loop, 0.9 g input

Fig. 8 - Average stress of central & corner isolators and hysteretic loops of central isolator

4. Conclusions

In this paper, a static test of an innovative three-dimensional isolator was conducted. And the seismic response of a three-dimensional isolated nuclear power plant was analysed. The main conclusions are as follows:

(1) A novel three-dimensional isolator in which rubber bearings were installed with inclination was introduced. The mechanical model of the proposed isolator was established. The loading stiffness are larger than the unloading stiffness due to friction sliding.

(2) A static test on the shear performance, compression performance, and bidirectional performance was conducted. The proposed isolator has stable hysteretic performance in both horizontal and vertical

directions. The horizontal deformation has little influence on the vertical properties. The horizontal and vertical performances can be considered independent.

(3) A three-dimensional design and seismic analysis of a nuclear power plant was accomplished. The proposed isolator can sufficiently protect nuclear structure as well as internal equipment under three-dimensional earthquake. The vertical responses of the three-dimensional isolators are stable and close considering additional rocking suppression system.

5. Acknowledgement

This work was supported by the Major National Science and Technology Projects (Grant No. 2017ZX06002003) and the National Natural Science Foundation of China (Grant No. 51778355 and 51778356)

6. References

[1] Architectural Society of Japan. Liu WG., Translation. (2003) Recommendation for the design of base isolated buildings. Seismological Press, Beijing, China. (in Chinese)

[2] Papazoglou A.J., Elnashai A.S. (1996) “Analytical and fileld evidence of the damaging effect of vertical earthquake ground motion,” Earthquake Engineering and Structural Dynamics, Vol. 25, pp1109 -1137.

[3] Fujita S, Kato E., Kashiwazaki A., et al. (1996) “Shake table tests on three-dimensional vibration isolation system comprising rubber bearing and oil spring,” Proceedings of 11th World Conference on Earthquake Engineering, Acapulco, Mexico.

[4] Garevski M., Kelly J. M., Zisi N. (2000) “Analysis of 3D vibrations of the base isolated school building ‘Pestalozzi’ by analytical and experimental approach,” Proceedings of the 12th WCEE, Auckland, New Zealand.

[5] Kato, A., et al. (2002) “A large Scale Ongoing R&D Project on Three-Dimensional Seismic Isolation for FBR in Japan,” 2002ASME PVP, Seismic Engineering, Vancouver, Canada.

[6] Seitaro O., Kyotada N., Michiaki S., Satoshi M. (2003) “Development of 3D Seismic Isolator using Metallic Bellows,” Transactions of the 17th International Conference on Structural Mechanics in Reactor Technology (SMiRT 17), Prague, Czech Republic

[7] Meng QL., Lin DQ., Zhang MZ. (2007) “Study on Three-Dimensional Isolated System in Shaking Table Test,” Journal of Earthquake Engineering and Engineering Vibration, Vol. 27, No. 3, pp116-120. (in Chinese).

[8] Liu HQ., Wang J.L. (2008) “The Shell Structure Earthquake Analysis based on the SMA 3D Base Isolator,” Proceedings of the Second International Forum on Advances in Structural Engineering, Dalian, China. (in Chinese).

[9] Zhang YS., et al. (2009) “Experimental Study on Mechanical Properties of Three-Dimensional Base Isolation and Overturn Resistance Device,” Engineering Mechanics, Vol. 26 No. Sup.I, pp124-129. (in Chinese).

[10] Tomizawa T, Takahashi O, Aida H, et al. (2012) “Vibration test in a Building named ‘Chisuikan’ using Three-dimensional Seismic Isolation System,” The 15th World Conference on Earthquake Engineering, Beijing, China.

[11] Jia JF., Ou JP., et al. (2012) “Mechanical performance tests of a novel three-dimensional isolation bearing,” Journal of Civil, Architectural & Environmental Engineering. Vol. 34, No. 1, pp29-34. (in Chinese).

[12] Wei LS., Liu LF., Liang HW. (2014) “Experimental study on three-dimensional seismic isolation,” China Civil Engineering Journal. Vol. 47, No. 3, pp33-38. (in Chinese).

[13] Liu WG., et al. (2018). “Static test and seismic dynamic response of an innovative 3D seismic isolation system”. Journal of Structural Engineering. Vol. 144, No. 12, pp04018212.

[14] Li ZX., et al. (2005) “Sensitivity Analysis for Floor Response Spectra of Nuclear Reactor Buildings”. Nuclear Power Engineering, Vol. 26, No. 1, pp44-45. (in Chinese)

[15] NRC (US Nuclear Regulatory Commission Office of Nuclear Regulatory Research). 2014. Regulatory guide 1.60 design response spectra for seismic design of nuclear power plants. Rockville, MD: NRC.

